

Contents lists available at [SciVerse ScienceDirect](http://SciVerse.Sciencedirect.com)

Icarus

journal homepage: www.elsevier.com/locate/icarus

New insights into the structure and chemistry of Titan's tholins via ^{13}C and ^{15}N solid state nuclear magnetic resonance spectroscopy

S. Derenne^{a,*}, C. Coelho^b, C. Anquetil^a, C. Szopa^c, A.S. Rahman^d, P.F. McMillan^d, F. Corà^d, C.J. Pickard^e, E. Quirico^f, C. Bonhomme^g^a Biogéochimie et Ecologie des Milieux Continentaux, UMR 7618 CNRS, UPMC, case courrier 120, 4 place Jussieu, 75252 Paris cedex 05, France^b Institut des Matériaux de Paris Centre, FR2482, UPMC, Collège de France, 11 place Marcelin Berthelot, 75231 Paris cedex 05, France^c Laboratoire Atmosphères, Milieux, Observations Spatiales, UPMC/Université de Versailles Saint Quentin, Verrières le Buisson, France,^d Christopher Ingold Laboratories, Department of Chemistry, University College London, 20 Gordon Street, London WC1H 0AJ, UK^e Department of Physics and Astronomy, University College London, Gower Street, London WC1E 6BT, UK^f Institut de Planétologie et d'Astrophysique de Grenoble, Université Grenoble 1/CNRS, 38041 Grenoble cedex 9, France^g Laboratoire de Chimie de la Matière Condensée de Paris, UMR 7574 CNRS, UPMC, Collège de France, 11 place Marcelin Berthelot, 75231 Paris cedex 05, France

ARTICLE INFO

Article history:

Received 21 November 2011

Revised 15 February 2012

Accepted 4 March 2012

Available online 10 March 2012

Keywords:

Cosmochemistry

Exobiology

Titan

Atmospheres, Chemistry

ABSTRACT

Tholins are complex C,N-containing organic compounds produced in the laboratory. They are considered to provide materials that are analogous to those responsible for the haze observed in Titan's atmosphere. These compounds present an astrobiological interest due to their ability to release amino acids upon hydrolysis. Their chemical structure has been investigated using a large number of techniques. However, to date no detailed nuclear magnetic resonance (NMR) study has been performed on these materials despite the high potential of this technique for investigating the environment of given nuclei. Here ^{13}C and ^{15}N solid state NMR spectroscopy was applied to obtain new insights into the chemical structure of tholins produced through plasma discharge in gaseous $\text{N}_2\text{—CH}_4$ mixtures designed to simulate the atmosphere of Titan. Due to the low natural abundance of these isotopes, a ^{13}C and ^{15}N -enriched tholin sample was synthesized using isotopically enriched gas precursors. Various pulse sequences including ^{13}C and ^{15}N single pulse, $^1\text{H}\text{—}^{13}\text{C}$ and $^1\text{H}\text{—}^{15}\text{N}$ cross-polarisation and $^1\text{H}\text{—}^{15}\text{N}\text{—}^{13}\text{C}$ double cross-polarisation were used. These techniques allowed complete characterisation of the chemical and structural environments of the carbon and nitrogen atoms. The NMR assignments were supplemented and confirmed by *ab initio* electronic structure calculations for model structures and molecular fragments.

© 2012 Elsevier Inc. All rights reserved.

1. Introduction

Titan, the largest moon of Saturn, is characterized by a dense atmosphere, mainly composed of N_2 (ca. 97%) and CH_4 (ca. 2%). In the upper atmosphere, methane and nitrogen molecules undergo dissociation under the influence of solar UV radiation and electron impacts, followed by recombination reactions leading to a large variety of organic molecules (Waite et al., 2007). Some of these compounds form a thick, orange-coloured haze composed of solid organic aerosols that subsequently fall to the surface or remain in suspension in the atmosphere.

To gain insight into the chemical composition and structural nature of these complex organic compounds, analogous materials are produced in the laboratory, in particular using plasma dis-

charge in gaseous $\text{N}_2\text{—CH}_4$ mixtures that are designed to simulate Titan's atmosphere (Coll et al., 1999; Imanaka et al., 2004; Szopa et al., 2006). These materials are commonly termed "Titan's tholins", derived from the Greek term for "muddy" (Sagan and Khare, 1979). Depending on the experimental conditions, their composition, structure and spectral properties can vary largely. Some tholins mimic the optical properties of Titan's aerosols in the visible range (Khare et al., 1984a). Furthermore, tholins present an interest for astrobiology as they were shown to release amino acids upon hydrolysis (Thompson and Sagan, 1989; Neish et al., 2009) and nucleobase after X-ray irradiation (Pilling et al., 2009).

Titan's tholins have been analysed using a wide variety of techniques ranging from bulk elemental analysis (McDonald et al., 1994; Coll et al., 1999; Sarker et al., 2003; Szopa et al., 2006; Quirico et al., 2008), pyrolysis (Khare et al., 1984b; Ehrenfreund et al., 1995; Coll et al., 1999; Hodyss, 2005; Szopa et al., 2006; McGuigan et al., 2006) and laser desorption mass spectrometry experiments (Somogyi et al., 2005; Ganesan et al., 2007; Imanaka and Smith,

* Corresponding author.

E-mail address: sylvie.derenne@upmc.fr (S. Derenne).

2010) to infrared absorption, visible, UV and near-IR Raman and luminescence spectroscopy (Sagan et al., 1993; McDonald et al., 1994; Khare et al., 2002; Imanaka et al., 2004; Bernard et al., 2006; Quirico et al., 2008; Ruiz-Bermejo et al., 2008, 2009; Carrasco et al., 2009), X-ray diffraction and high resolution transmission electron microscopy (Quirico et al., 2008). The fraction of the tholins that was soluble in normal or deuterated solvents, or in the presence of crown ethers in certain cases, has been studied using electrospray ionization mass spectrometry (Sarker et al., 2003; Somogyi et al., 2005; Hodyss, 2005; Carrasco et al., 2009; Pernot et al., 2010) and gas chromatography coupled to mass spectrometry (Hodyss, 2005).

All these studies have provided a wealth of information about potential functional groups and structural building blocks present within the tholin samples. Taken together, the results converge on a structure based on a $C_xH_yN_z$ chemistry, that can contain various oligomeric and polymeric chain or ring units, and containing a variety of C–C, C–N, N–H, etc. single or multiple bonds. It is now necessary to build on that information to refine the chemical and structural models for the Titan model tholins. Here we investigate these complex materials using solid state nuclear magnetic resonance (NMR) techniques.

NMR is a powerful tool for structure determination of complex organic molecules and solid state species, providing detailed element-specific information about local structure and chemical environments. In the present study, we used solid state NMR techniques to investigate the carbon and nitrogen bonding environments in a ^{13}C - and ^{15}N -enriched sample recovered from the plasma discharge synthesis experiment. Solid state NMR was preferred to solution state due to the low solubility of the studied sample (Carrasco et al., 2009). A preliminary solid state ^{13}C NMR study of Titan tholins was performed by Sagan et al. (1993) but no spectrum was published and it only reported that 25% of the carbon atoms were unsaturated. We used techniques of isotopic enrichment and cross-polarisation (CP) to enhance the signal intensity combined with magic angle spinning (MAS) to reduce the broadening of the NMR peaks. We also compare the results with selected data from a parallel study of graphitic carbon nitride materials that are being developed for photocatalysis and other optoelectronic applications (Bojdys et al., 2008; Wang et al., 2009; McMillan et al., 2009).

Quantitative NMR data related to structure can be obtained by measuring relative peak intensities obtained through direct polarisation using a single pulse (SP) sequence. However, due to the low natural abundance and NMR sensitivity of the main isotopes of interest, especially ^{15}N , such SP spectra often have a low signal to noise ratio. To overcome this, tholins were synthesized from isotopically enriched mixtures using pure $^{13}CH_4$ and 30% enriched $^{15}N_2$. Techniques using CP pulse sequences can be used to enhance the signal intensity (Schaefer and Stejskal, 1976). These experiments involve excitation of the most abundant and NMR sensitive spins within the sample (i.e., 1H nuclei in the case of the $C_xN_yH_z$ tholins) and magnetisation is transferred towards less abundant spins of interest (i.e., ^{13}C or ^{15}N). During the transfer process characterized by the contact time, the ^{13}C or ^{15}N magnetisation increases exponentially; however, the protons are simultaneously relaxing during this period, resulting in a decrease in the overall magnetisation. The magnetisation transfer and relaxation rates depend on the local ^{13}C or ^{15}N environments and are influenced by the proximity to as well as the number of the excited protons, along with any molecular motions present in the system. Here we present CP spectra obtained as a function of the contact time. The analysis of these results provides new information on the spatial distribution of C, N and H nuclei within the materials.

Linkages between carbon and nitrogen atoms were also investigated by NMR, using the double 1H – ^{15}N – ^{13}C CP technique, in

which 1H magnetisation is first transferred to ^{15}N nuclei which are then allowed to evolve and their magnetisation is further transferred to ^{13}C (Schaefer et al., 1979). As a result, using the double CP sequence, only the ^{13}C signals of those carbons that are closely coupled to ^{15}N nuclei are observable and the intensity of the signal varies according to the strength of their coupling. The key parameters here are therefore the 1H – ^{15}N and ^{15}N – ^{13}C contact times. One- and two-dimensional NMR experiments can be conducted, providing additional information on the C,N,H arrangements within the sample (Fujiwara et al., 1995). Double CP spectra were recorded using various 1H – ^{15}N and ^{15}N – ^{13}C contact times on tholin.

One main question to be addressed concerns the structural assignment of ^{13}C and ^{15}N NMR shifts obtained from the SP and CP experiments. Usually these attributions are carried out based on knowledge of functional groups within the existing NMR large data base for organic compounds. These provide useful structural analysis tools but do not always provide reliable ways to interpret the potentially unusual C–N–H bonding or molecular fragments present within tholins produced in the laboratory. Here we complemented our experimental study by carrying out *ab initio* predictions of ^{13}C and ^{15}N NMR shifts for molecular models and fragments using electronic structure methods in order to support and aid in the structural interpretation of our experimental data.

2. Experimental

2.1. Samples

The tholin sample for the solid state NMR study was produced within the PAMPRE experiment using a N_2 – CH_4 gaseous mixture submitted to a plasma discharge (Szopa et al., 2006). The gaseous mixture contained $2.00 \pm 0.06\%$ of pure ^{13}C -labelled methane (Eurisotop, Saclay, France) in N_2 isotopically enriched with 30% of $^{15}N_2$ nitrogen (Eurisotope, Fr.). That enrichment procedure enabled us to obtain single pulse (SP) ^{13}C and ^{15}N NMR spectra in the present study. The operating conditions were 0.9 mbar total pressure, ambient laboratory temperature, and a 30 W injected radio-frequency power. The elemental composition had H/C and N/C atomic ratios of 1.1 and 0.77, respectively (Quirico et al., 2008).

2.2. NMR experiments and first principles calculations

The ^{13}C and ^{15}N -enriched tholin material prepared by PAMPRE was examined by solid state NMR using a Bruker AVANCE III 700 spectrometer at $B_0 = 16.4$ T with $\nu_0(^{13}C) = 176.07$ MHz and $\nu_0(^{15}N) = 70.95$ MHz, with a 3.2 mm triple resonance Bruker MAS probe, spinning at 22 kHz. Samples were spun at the magic angle using ZrO_2 rotors. ^{13}C and ^{15}N NMR chemical shifts were calibrated to glycine enriched in ^{13}C and ^{15}N and referenced with respect to TMS and nitromethane respectively. Full experimental details (e.g., number of scans (NS), recycle time (RD), etc.) are shown in the figure captions. Decomposition of spectra was performed using the dmfit software (Massiot et al., 2002).

Electronic structure calculations were carried out to support and confirm the NMR assignments. Because many of the candidate structures appear within solid state crystalline or nanocrystalline materials we chose to use the CASTEP code (version 5.5), which uses planewave basis functions to model the electronic wavefunction in the Kohn–Sham formulation of density functional theory (DFT) (Clark et al., 2005). CASTEP enables a consistent calculation of NMR shifts for molecules and solid-state systems and provides a way to discriminate between the individual atom environments predicted to occur within the tholins at various C:N:H ratios. To model NMR shifts for certain species, individual molecules or

molecular fragments were also examined using CASTEP. In these cases a large unit cell was constructed containing a single molecular fragment that was sufficiently distant from any neighbours to eliminate possible interaction effects. We have recently tested such an approach comparing CASTEP with molecular NMR shift calculations (using the GAUSSIAN 09 code: Frisch et al., 2009) (Aliev et al., 2011). All calculations used the PBE exchange correlation functional (Perdew et al., 1999) with ultrasoft pseudopotentials for the atoms involved (Vanderbilt, 1990). Prior to the calculation of NMR shielding parameters, full geometry optimizations were carried out, with all atoms and unit cell parameters allowed to relax according to the determined crystalline structures. Molecular systems simulated using periodic boundary conditions were fully optimised within a fixed unit cell of sufficient size to ensure that interactions between the periodic images of the molecule were negligible. A k-point spacing of 0.04 \AA^{-1} and cut-off energy of 700 eV provided suitable convergence for the various C–N–H structures considered, including pyridine, pyrimidine etc. and substituted triazines and their derivatives such as melon and melem (Jurgens et al., 2003; Bojdys et al., 2008). The optimized geometries were then used in NMR shielding calculations using the “gauge including projector augmented-wave” (GIPAW) method (Pickard and Mauri, 2001; Yates et al., 2007). Our calculations for the NMR reference standards tetramethylsilane (TMS) and nitromethane (CH_3NO_2) gave the following isotropic shielding parameters (σ_{iso}) for ^{13}C and ^{15}N : TMS (^{13}C) $\sigma_{\text{iso}} = 178.2$ ppm and nitromethane (^{15}N) $\sigma_{\text{iso}} = -165.5$ ppm. For the C–N–H structures investigated, the calculated isotropic shielding parameters (σ_{iso}) were subtracted from the reference values in order to convert them into chemical shifts (δ_{iso}) in ppm units relative to TMS and nitromethane for direct comparison with experiment (Table 1).

3. Results and discussion

3.1. Characterisation of carbon chemical environments using ^{13}C NMR

The solid state ^{13}C MAS single pulse (SP) spectrum of the tholin shows a dominant peak at 140–180 ppm that contains at least two contributions corresponding to sp^2 -bonded carbon atoms (Fig. 1a). This region can contain substantial contributions from heterocyclic aromatic species containing triazine (C_3N_3) rings and/or heptazine (C_6N_7) units, as well as carbons involved in imino groups. These possibilities are discussed below. There is also a broad signal extending between 5 and 100 ppm due to aliphatic carbons, and a well-resolved peak at 121 ppm that is characteristic of nitrile species ($-\text{C}\equiv\text{N}$) (Fig. 1a). Those assignments are supported by our first principles calculations (Table 1). Indeed, the DFT calculation results indicate values for ^{13}C shifts for the nitrile carbon in $\text{H}-\text{C}\equiv\text{N}$ and $\text{CH}_3\text{C}\equiv\text{N}$ to be 120 and 124 ppm, respectively (Table 1). The effect of substitution of H by other functional groups in $\text{R}-\text{C}\equiv\text{N}$ systems including an aromatic moiety was also investigated, and it resulted in a relatively small variation of the chemical shift (Table 1). We also investigated the effects of substituting the H substituents within melamine and triazine derivatives, where the ^{13}C chemical shifts for the attached carbons were predicted to occur at 126 ppm and 124 ppm respectively. The aromatic carbons occurred in the region of 120–129 ppm for melamine and 129–133 ppm for triazine. We also investigated the effect of adding an amine function attached to the nitrile group ($\text{N}\equiv\text{C}-\text{NH}_2$): here we expect that the chemical shift would lie at approximately 118 ppm (Table 1).

To assess the relative contributions of the different types of carbon species, the SP spectrum was decomposed into contributions using a Gaussian fitting procedure (Fig. 1a). A minimum number of lines were used to obtain a satisfactory fit, taking into account

the spinning side bands. This decomposition indicates that 60% of the carbons are sp^2 , 11% correspond to nitrile species and 29% to aliphatic carbons.

In order to gain further insight into the detailed peak assignments, variable contact time (t_{CP}) $^1\text{H}-^{13}\text{C}$ cross-polarisation (CP) experiments were performed (Fig. 1b). The spectra were initially recorded at spinning speeds of 14 and 22 kHz to identify possible contributions from spinning side bands. None were observable in the 22 kHz spectrum and so this spinning rate was chosen for all subsequent experiments.

When compared with the SP spectrum, we observe an increase in intensity of the 0–100 ppm signal at short contact time ($t_{\text{CP}} = 0.5$ ms) indicating that the aliphatic carbons are mainly protonated. When the contact time is increased from 0.5 to 5 ms, the relative abundance of this signal decreases rapidly relative to that of the 140–200 ppm signal, indicating a lower degree of protonation for the sp^2 carbons than for the aliphatic sp^3 sites.


The aliphatic range is characterized by an asymmetric feature centered at around 44 ppm, with main shoulders occurring at 26 and 31 ppm (Fig. 1). When the contact time is varied between 0.5 and 5 ms, a regular increase in the intensity of the shoulder at 26 ppm and to a lesser extent that at 31 ppm is observed, compared with the overall maximum near 44 ppm, indicating differences in the CP dynamics (Fig. 1b). Based on their chemical shift values, the most deshielded carbons are most likely linked to nitrogen, as found in amine groups ($-\text{C}-\text{N}$). The most shielded carbons most probably correspond to methyl groups ($-\text{CH}_3$) as it is known that their pseudo-free rotation partially averages the CP process and the chemical shifts of methyl groups substituting C atoms adjacent to N in pyrimidine **I** or triazine **II** occur in the 20–27 ppm range (Stothers, 1972). Values in the same range were obtained for the chemical shift of methyl groups in various molecules as the result of our DFT calculations (Table 1).

Within the envelope of the 140–200 ppm signal, two peaks are clearly distinguished at 160 and 168 ppm. Carbon atoms responsible for the 168 ppm peak are evidently more protonated than those responsible for the 160 ppm signal based on the variable contact time (t_{CP}) experiments. Based on their chemical shift, these sp^2 carbons may be linked to nitrogen as found in imine groups or in aromatic heterocyclic units. Indeed, C adjacent to N in six-membered heterocycles including triazine and its derivatives have chemical shifts ranging between 140 and 170 ppm and the resonances become more deshielded when the C atoms are substituted by aliphatic or amino groups (Stothers, 1972). For example, C atoms adjacent to N in pyridine **III** and pyrimidine **I** exhibit chemical shifts of 151 and 158 ppm, respectively, and these resonances shift to 160 and 167 when the heterocycle is substituted by a methyl or an amino group. C in triazine **II** and in its triamino derivative (i.e., melamine) is characterized by a chemical shift of 167 ppm. This is further supported by our theoretical calculations (Table 1). Likewise, the ^{13}C NMR spectrum of melem (triaminoheptazine) **IV** shows a peak at 165 ppm for the C atom bearing the amino group, compared with 155 ppm for the other ^{13}C resonances in the structure (Jurgens et al., 2003; Table 1). The central carbon atoms in dicyandiamide ($\text{C}_2\text{N}_4\text{H}_4$: $\text{NH}_2-\text{C}(=\text{NH})-\text{NH}-\text{C}\equiv\text{N}$) exhibit a ^{13}C chemical shift at 163 ppm (Cardamone et al., 2006). The theoretical results combined with experimental observations indicate that it is not possible to discriminate between imine carbons ($\text{C}=\text{N}$) occurring in straight chains vs heterocyclic environments using ^{13}C NMR spectroscopy alone, however.

^{13}C resonances in the 155–170 ppm range have been recorded for a nanocrystalline graphitic carbon nitride material obtained by reaction between melamine and cyanuric chloride under high pressure-high temperature conditions (Zhang et al., 2001). The resulting solid had a composition $\text{C}_6\text{N}_9\text{H}_3\cdot\text{HCl}$ (or $[\text{C}_6\text{N}_9\text{H}_4]^+\text{Cl}^-$) with Cl atoms or Cl^- ions included in the structure derived from

Table 1

Summary of the occurrence of the structural units of the tholin sample with the experimental and theoretical range.

| Functional group | Experimental chemical shifts (ppm) | | Occurrence in tholin sample | Justification from experimental data | Structures simulated theoretically | Theoretical chemical shifts (ppm) | |
|------------------------------------------------------------------------------------------------------|------------------------------------|-----------------|------------------------------------------------------------------------------------------------------|----------------------------------------------------------------------------|-------------------------------------------------------------------------------|-----------------------------------|------------------|
| | ¹³ C | ¹⁵ N | | | | ¹³ C | ¹⁵ N |
| Nitriles —C≡N | 121 | −134 | Present | ¹³ C and ¹⁵ N chemical shift, CP behaviour | H—C≡N | 120 | −144 |
| | | | | | H ₃ C—C≡N | 124 | −131 |
| | | | | | H ₂ N—C≡N | 118 | −184 |
| | | | | | Benzene—C≡N | 114 | −111 |
| | | | | | Melamine—C≡N ^A | 126 | −137 |
| | | | | | Triazine—C≡N ^A | 124 | −108 |
| Amines —C—N | 44 | −300 to −330 | Present , most likely linked to sp ² -bonded C possibly in heterocyclic structures | ¹³ C and ¹⁵ N chemical shift, 1D double CP behaviour | Melamine (C—NH ₂) | 165 | −329 |
| | | | | | Melem IV (C—NH ₂) | 162 | −313 |
| | | | | | Molecule resulting from the fusion of 3 heptazines | 161–163 | −304 |
| | | | | | H ₃ C—NH ₂ | 30 | −388 |
| Methyl —CH ₃ | 26 | – | Present | ¹³ C chemical shift, CP behaviour | H ₃ C—NH ₂ | 30 | – |
| | | | | | H ₃ C—C≡N | 2 | – |
| | | | | | H ₃ C—N=C=N—CH ₃ | 34 | – |
| | | | | | H ₃ C—N≡C | 28 | – |
| | | | | | Hexamethylbenzene | 18 | – |
| | | | | | | | |
| sp ² carbons, imines C=C and/or C=N | 140–180 | −185 to −285 | Present | ¹³ C and ¹⁵ N chemical shift | Triazine | 168 | −95 |
| | | | | | Melamine | 165 | −219 |
| Isocyano —N≡C | 160 | −200 | <i>Possible but minor</i> | ¹³ C and ¹⁵ N chemical shift | H—N≡C | 175 | −240 |
| | | | | | H ₃ C—N≡C | 165 | −227 |
| | | | | | Melamine—N≡C ^B | 161 | −188 |
| | | | | | Triazine—N≡C ^C | 180 | −193 |
| Heterocyclic amine  | – | −356 | <i>Possible</i> | ¹⁵ N chemical shift | Hexahydrotriazine | 61 | −334 |
| | | | | | Hexahydropyridine | 29–51 | −336 |
| | | | | | Hexahydropyrimidine | 35–67 | −327 |
| NH ₄ ⁺ , NH ₂ —NH ₃ ⁺ | – | −356 | <i>Possible</i> | ¹⁵ N chemical shift | NH ₄ ⁺ Cl [−] | – | −350 |
| Carbodiimide —N=C=N— | 140 | −280 to −300 | <i>Possible but minor</i> | ¹³ C and ¹⁵ N chemical shift | H—N=C=N—H | 145 | −324 |
| | | | | | H ₃ C—N=C=N—CH ₃ | 130 | −319 |
| C=N—C≡N | | | <i>Possible</i> | Double CP experiment | H ₂ C ^a =N ^a —C ^b ≡N ^b | 180 ^a | −66 ^a |
| | | | | | | 122 ^b | −96 ^b |
| Heptazine (see structure IV) | ca.160 | −185 and −240 | <i>Possible</i> | ¹³ C and ¹⁵ N chemical shift | H ₂ N—C 3NC (outer N) | 162 | −313 |
| | | | | | 3CN (central N) | 154 | −198 |
| | | | | | | 154 | −238 |
| Aromatic hydrocarbons | 100–140 | – | <i>Possible but minor and mostly non-protonated</i> | ¹³ C chemical shift, CP behaviour | Benzene | 128 | – |
| | | | | | Hexamethylbenzene | 131 | – |
| Hydrazines R ₁ R ₂ N—N—R ₃ R ₄ | 150 | −275 to −330 | <i>Possible but minor</i> | ¹³ C and ¹⁵ N chemical shift | – | – | – |
| Hydrazones R ₁ R ₂ N=N=CR ₃ R ₄ | | −20 | Absent | ¹⁵ N chemical shift | – | – | – |
| Diazo compounds R ₁ R ₂ C=N=N | | −5 to −65 | Absent | ¹⁵ N chemical shift | – | – | – |

^{a,b} Refers to the corresponding C and N atoms in the associated structure.^A H substitution with C≡N.^B NH₂ substitution with N≡C.^C H substitution with N≡C.

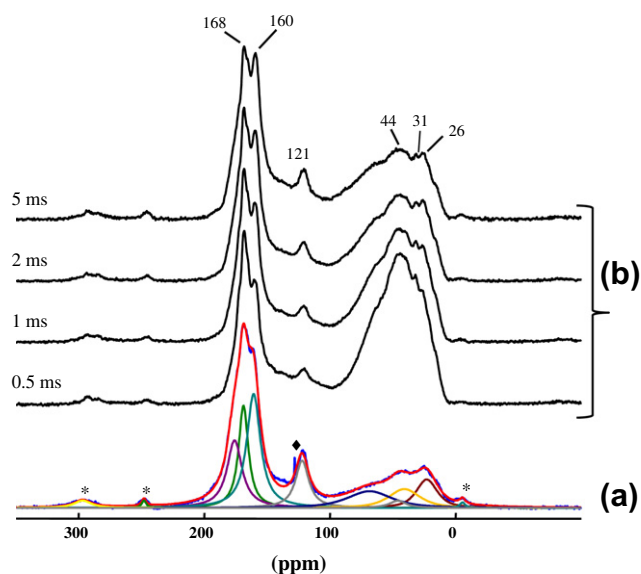


Fig. 1. (a) ^{13}C MAS NMR spectra of tholin sample (NS = 40, RD = 60 s) showing the decomposition of the spectrum. (b) ^{13}C CP MAS NMR spectra of tholin sample (NS = 112, RD = 5s) recorded at t_{CP} = 0.5, 1, 2 and 5 ms from bottom to top (* spinning side bands, \blacklozenge artefact).

the synthesis along with additional N–H groups: the structure contains triazine units linked by bridging imido/amido groups to form large ($\text{C}_{12}\text{N}_{12}$) voids in the graphitic layers surrounding the Cl species (Zhang et al., 2001; McMillan et al., 2009). Two main resonances were observed at 166 and 159 ppm. The higher ppm value was assigned to C atoms involved in the triazine (C_3N_3) rings, as found in melamine and other structures. The lower ppm signal was attributed to C atoms linked to bridging –NH– units. Those assignments agree with results of our first principles calculations (Table 1). Recently we have also studied other graphitic C,N materials produced by ionothermal/solvothermal methods that are thought to contain heptazine units (i.e., three fused triazine rings sharing a central N atom) (Bojdys et al., 2008; Wang et al., 2009). These materials also exhibit the main 166 ppm ^{13}C resonance due to triazine rings accompanied by a second feature at approximately 155 ppm that appears for those C atoms linked to the central triply-bridging N atom (Rahman et al., in preparation).

Our first principles calculations support these assignments for various species that are possibly or probably present within the tholin sample. For melamine, the isotropic ^{13}C NMR shift occurs at 165 ppm in the molecular solid, and in an extended graphitic melamine framework modelled in this study the chemical shift is calculated to occur at 162 ppm. For molecular melem units, there are two C environments occurring in a 1:1 ratio, that are attached to two nitrogen atoms and amino group, and those that are attached to three N atoms including the central atom providing the bonding between triazine units, respectively. The C atom bearing the amino group gives a calculated shift at 162 ppm, whereas the other C atomic environment results in a shift at 154 ppm (Table 1). Within an extended graphitic system based on polymerised melem units, these values occur at 162 and 156 ppm respectively. In these structural units, an additional third C environment attached to the imido bridging group also gives rise to a chemical shift occurring at 164 ppm, so that it is impossible for the ^{13}C NMR results to distinguish between the two.

Other potential contributions to the 140–180 ppm peak result from the possible presence of isocyano groups ($-\text{N}=\text{C}$) and carbodiimide moieties ($-\text{N}=\text{C}=\text{N}-$). These alternative assignments would be consistent with the low CP dynamics revealed by the

variable contact time experiments. They are further discussed and elucidated with reference to the $^1\text{H}-^{15}\text{N}$ cross-polarisation experiments described below.

The broad signal between 100 and 140 ppm likely indicates a small contribution from other aromatic carbon species present in the sample. DFT calculation results indicate ^{13}C values around 130 ppm for benzene and its hexamethyl homologue (Table 1). The behaviour of the 100–140 ppm signal in the variable contact time experiment is similar to that of the nitrile peak, suggesting that these C sites are mainly non-protonated.

To summarise, these ^{13}C NMR experiments combined with the first principles theory predictions reveal the presence of mainly protonated aliphatic carbons present within the tholin sample. Some of the aliphatic carbons are linked to N incorporated within amine functional groups and others are clearly involved in methyl species. The occurrence of nitrile groups within the tholin sample is also evident. The dominant ^{13}C NMR signal can be assigned to sp^2 carbons linked to N within heterocyclic units or imine functions although a contribution from isocyano groups or carbodiimide moieties cannot be excluded at this stage of the analysis. A minor contribution of non-protonated aromatic carbons could also be present.

3.2. Characterisation of nitrogen chemical environments using ^{15}N NMR

The single pulse solid state ^{15}N MAS data recorded for the tholin sample presents a quite complex spectrum (Fig. 2a). A main broad peak occurs between –230 and –340 ppm with maxima at –272 ppm and –304 ppm, along with two shoulders at –330 and –256 ppm. An additional broad signal occurs throughout the –160 to –230 ppm range with maxima near –185 ppm and –170 ppm, as well as an additional well-resolved peak at –134 ppm (Fig. 2a). The peak at –134 ppm corresponds to positions usually assigned to nitrile species, whereas –330 ppm is a typical chemical shift for amines. Both of these species were indicated to be present in the tholin sample from ^{13}C SP and CP MAS NMR spectroscopy discussed above. Their assignment is supported by first principles calculations (Table 1).

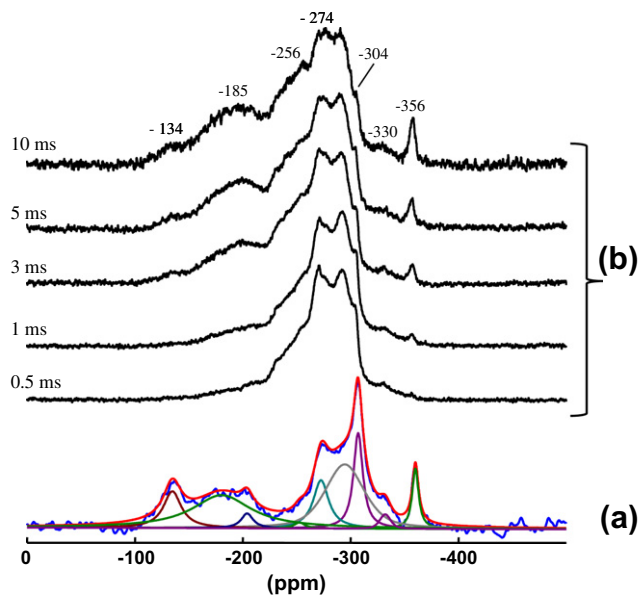


Fig. 2. (a) ^{15}N MAS NMR spectra of tholin sample (NS = 1908, RD = 180 s) showing the decomposition of the spectrum. (b) ^{15}N CP MAS NMR spectra of tholin sample (NS = 13,500, RD = 5 s) recorded at t_{CP} = 0.5, 1, 3, 5 and 10 ms from bottom to top.

There is also a sharp peak at -356 ppm. This falls within an unusual range for ^{15}N chemical shifts. Heterocyclic amines might account for this observation as supported by literature data (Martin et al., 1981) although the present DFT calculations result in slightly higher chemical shifts (Table 1). However, the corresponding ^{13}C chemical shifts fall in the 30 – 70 ppm range, reported above for aliphatic carbons. Ammonium or hydrazinium ions located close to polynitrogen chains such as azides have also been reported to exhibit such anomalously negative chemical shift values (Klapötke and Stierstorfer, 2009; Klapötke et al., 2009). The low efficiency of CP dynamics for the peak at -356 ppm observed in this study may be explained by the presence of NH_4^+ groups in the sample combined with their expected rotational motion. That assignment is supported by the theoretical results that predict a ^{15}N shift for ammonium species at -350 ppm (Table 1).

Based on ^{13}C chemical shift data, contributions from six-membered heterocycles were considered to be present. This might initially seem at variance with the observed ^{15}N chemical shifts, as values of -63 ppm, -85 ppm and -103 ppm have been reported for pyridine **III**, pyrimidine **I** and triazine **II**, respectively. However, it has also been observed that substitution by amino groups induces a strong shift towards more negative values (-190 and -207 ppm for 2,4,6 triamino-pyrimidine and -triazine, respectively) and that the chemical shift for the amino group in such compounds occurs at around -300 ppm (Martin et al., 1981). This is supported by our first principles calculations which indicate that the $-\text{NH}_2$ groups in melamine give rise to a chemical shift at -329 ppm whereas the aromatic N species incorporated in the triazine rings leads to a signal at -219 ppm (Table 1). Similar shifts were reported for 2-*exo*-cyanomethylene substituted quinoxalines **VI** and their cyanoimino analogues **VII** where values of -274 and -285 ppm were recorded for the N atoms (Benassi et al., 2000). Interestingly, the carbon atom located between the two N atoms in the heterocycle exhibited ^{13}C shifts of 156 – 158 ppm, similar to the values observed for the tholin sample (Fig. 1).

^{15}N chemical shifts at around -280 ppm have also been reported to occur for N atoms contained within carbodiimide structures ($-\text{N}=\text{C}=\text{N}-$), that become shifted to -297 ppm when an additional amino group is present on the side chain (Martin et al., 1981). However, in such structures the corresponding chemical shift of the central C atom occurs at ca. 140 ppm. These chemical shifts are supported by first principles calculations (Table 1). The low abundance of the signal in ^{13}C CP MAS points to, at most, a minor contribution of carbodiimide functions.

From the ^{13}C NMR spectrum, a contribution of isocyanate groups could be considered. We therefore investigated the corresponding ^{15}N chemical shifts. A value of -204 ppm was experimentally obtained for diisocyanobenzene and first principles calculations led to values ranging from -188 to -240 ppm for ^{15}N and 161 – 180 ppm for ^{13}C . Isocyanate groups may therefore contribute to a part of the NMR signal.

^{13}C chemical shifts recorded for melem **IV** containing triazine and heptazine units were similar to those observed for the tholin sample (Jurgens et al., 2003), and so we examined the corresponding ^{15}N shifts for molecular units associated with these species. The N atoms located at the periphery of the condensed rings give rise to an intense signal at -200 ppm, whereas the central N is observed to resonate at -234 ppm (Jurgens et al., 2003). Amino groups from local groups such as those existing in melem are also detected at -267 and -281 ppm (Jurgens et al., 2003). In the present work, the simulated ^{15}N chemical shifts for the heptazine (melem) molecular unit yielded three values, with the amine group occurring at -313 ppm, the central N at -238 ppm and outer N atoms at -198 ppm (Table 1). These results are consistent with the idea that heptazine units are present within the tholin sample. It must

be noted that similar values are obtained when the fusion of three heptazine moieties is considered (Table 1).

^{15}N CP MAS experiments were performed at variable contact times ($t_{\text{CP}} = 0.5$ – 10 ms) (Fig. 2b). The results indicate the most efficient CP dynamics for ^{15}N resonances occurring in the -270 to -295 ppm range, compared with the resonances in the -134 to -198 ppm range that showed a rather slow polarisation transfer. This is consistent with the assignments of the -134 ppm peak to nitrile groups and of at least a part of the -200 ppm peak to isocyanate groups.

These ^{15}N NMR experiments confirm the presence of nitrile and amine groups in the tholin sample. The occurrence of isocyanate groups is consistent with the ^{13}C NMR data, along with a low contribution of carbodiimide entities to the NMR spectra. The occurrence of amino-substituted six-membered heterocycles is supported by resonances both in the range of the amino substituents and of the imino functions from the rings, although other types of substituents (such as some bearing cyano groups) might also be present.

Decomposition of the SP spectrum into Gaussian components indicates that ca. 56% of the ^{15}N signal is observed between -230 and -340 ppm and 29% between -160 and -230 ppm. These resonances can be mostly assigned to amino groups (the more shielded area) located on imino groups (the less shielded area) possibly in heterocycles (triazine- or heptazine-like environments). The signal at -134 ppm, assigned to nitrile groups, accounts for 9% of the ^{15}N signal. This nitrile contribution is consistent with that (11%) derived from the ^{13}C NMR spectrum (Fig. 1a), when taking into account the N/C atomic ratio of the tholin sample. Finally, the neat signal at -356 ppm that we assign to the presence of NH_4^+ species or heterocyclic amines represents 6% of the N atoms.

3.3. N–C interactions studied via ^1H – ^{15}N – ^{13}C double CP-MAS NMR

3.3.1. One-dimensional ^1H – ^{15}N – ^{13}C double CP experiments

To specify further the linkages occurring between N and C centres in the tholin sample, ^1H – ^{15}N – ^{13}C double CP experiments were performed. Based on our previous experience obtained with the ^{15}N CP MAS spectra above, we selected ^1H – ^{15}N contact times at 0.5 and 5 ms. With the lower t_{C} value, the spectrum is chiefly composed of the main signal between -220 and -310 ppm, whereas the full spectral signal is observed at 5 ms. A variable ^{15}N – ^{13}C contact time experiment (Fig. 3) was then performed to highlight the N–C coupling characteristics and to select the most appropriate values for the 2D NMR experiments.

For ^1H – ^{15}N contact (t_{CP1}) experiments carried out at 0.5 ms, three values were selected for ^{15}N – ^{13}C contact times (t_{CP2}), namely 1 , 5 and 20 ms (Fig. 3a). At the lowest ^{15}N – ^{13}C contact time, the peak at 160 ppm is already most intense, indicating a stronger ^{15}N – ^{13}C coupling than for the C resonating at 168 ppm. Consistent with that result, the intensity of the ^{13}C peak at 168 ppm is higher than the 160 ppm one for a long ^{15}N – ^{13}C contact time (Fig. 3a). As expected, a weak resonance is observed between 5 and 100 ppm corresponding to aliphatic carbons located far from the N atoms. The nitrile carbons resonating at 121 ppm are clearly detected at longer contact time.

When using 5 ms as ^1H – ^{15}N contact time (t_{CP1}), we observed the same relative behaviour of the peak at 160 ppm with respect to that at 168 ppm (Fig. 3b). A broad signal is observed at 60 – 80 ppm using 5 ms as ^1H – ^{15}N contact time, but this it is not detected with 0.5 ms contact time. This is consistent with the assignment of this signal to amine groups, as N from amines is generally difficult to detect in ^{15}N CP MAS with short contact time conditions.

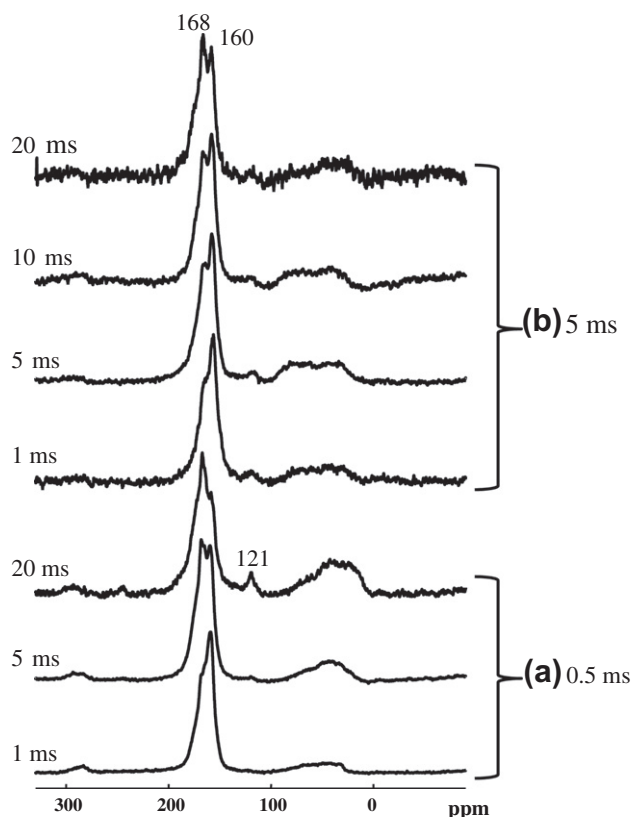


Fig. 3. ^1H – ^{15}N – ^{13}C CP MAS NMR spectra of tholin sample (NS = 16,116, RD = 5 s). (a) $t_{\text{CP1}} = 0.5$ ms and $t_{\text{CP2}} = 1, 5$ and 20 ms from bottom to top. (b) $t_{\text{CP1}} = 5$ ms and $t_{\text{CP2}} = 1.5, 10$ and 20 ms from bottom to top.

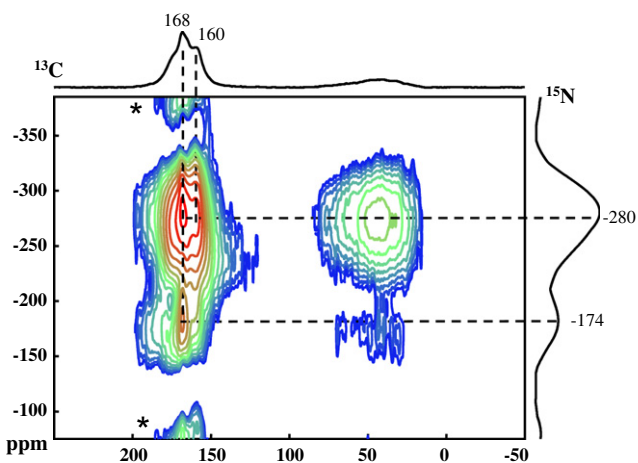


Fig. 4. 2D ^1H – ^{15}N – ^{13}C CP MAS NMR spectra of tholin sample (NS = 5056, states mode with 8 t_1 increments, RD = 5s, $t_{\text{CP1}} = 5$ ms, $t_{\text{CP2}} = 5$ ms) (* probably spinning side bands).

3.3.2. Two-dimensional ^1H – ^{15}N – ^{13}C double CP experiments

Following on from the double CP experiments described above, we ran two-dimensional spectra with two (^1H – ^{15}N , ^{15}N – ^{13}C) couples of contact times, namely (5, 5) and (0.5, 5) ms (Figs. 4 and 5). For the (0.5, 5) couple we ran spectra using recycle times of 3 and 5 s. It is clearly apparent that not all the C atoms are detected with the shorter recycle time and that using 3 s strongly

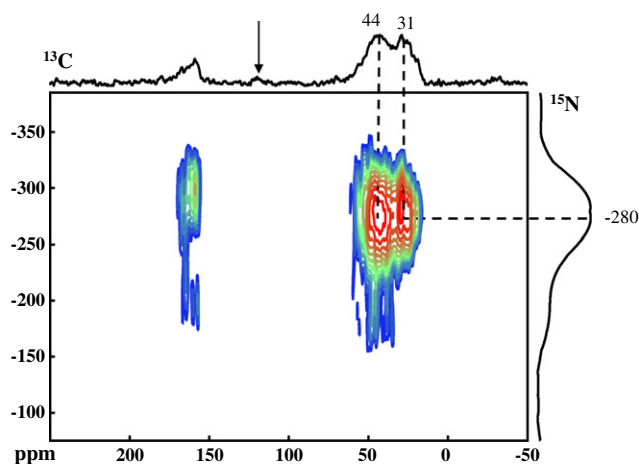


Fig. 5. 2D ^1H – ^{15}N – ^{13}C CP MAS NMR spectra of tholin sample (NS = 9600, states mode with 8 t_1 increments, RD = 3 s, $t_{\text{CP1}} = 0.5$ ms, $t_{\text{CP2}} = 5$ ms).

enhances the contribution from aliphatic carbons. The short delay time was then used to analyse the coupling with this type of C atoms.

The 2D spectrum recorded with $t_{\text{CP1}} = 5$ ms and $t_{\text{CP2}} = 5$ ms and a recycle time of 5 s (Fig. 4) clearly shows the coupling between the C atoms resonating at 168 ppm with the N atoms at -280 ppm and to a lesser extent with N at -174 ppm. In contrast, C centres at 160 ppm are only correlated with the N contributions from the main ^{15}N peak at -282 ppm. When the aliphatic carbons are considered, two types are distinguished at 31 and 44 ppm, and both are coupled with the broad N signal around -278 ppm.

A higher resolution of the aliphatic area is obtained with the spectrum recorded with a recycle time of 3 s and 0.5 and 5 ms as ^1H – ^{15}N and ^{15}N – ^{13}C contact times, respectively, clearly showing that the 31 ppm C are coupled with N at -280 ppm whereas the N which are coupled with C at 44 ppm are shifted towards -278 ppm (Fig. 5). It also clearly shows a correlation between C at 26 ppm and N at -278 ppm. A small correlation signal can be seen on the ^{13}C axis projection at 120 ppm (Fig. 5, arrow). When decreasing the gain factors within the map, a very low intensity spot can be detected, revealing a coupling between these carbons (involved in nitrile groups) and N atoms at -280 ppm, hence the possible presence of a $\text{C}=\text{N}-\text{C}\equiv\text{N}$ moiety. A similar low intensity signal was also detected when using a recycle time of 3 s and 5 ms for both ^1H – ^{15}N and ^{15}N – ^{13}C contact times. Such a low level of detection for this coupling can be partly explained by the slow polarisation of the nitrile group due to its lack of bonded H atoms.

It must be noted that C atoms that are more shielded than 20 ppm are never detected in these double CP experiments, consistent with aliphatic C not linked to N atoms. When the most deshielded aliphatic carbons are considered in the analysis, their behaviour in 1-D CP NMR (Fig. 3b) suggests a coupling with N but no corresponding spot can be seen in 2-D experiments. Similarly, no correlation is observed with the N at -330 ppm, although this is assumed to correspond to amino groups. This may be the result of both the low abundance of this type of N containing centres and the low ^{15}N – ^{13}C coupling constant. Similarly, no correlation is observable between N atoms resonating at -304 ppm and neighbouring C atoms likely because this N peak is barely distinguishable from the main signal when using the CP sequence. Finally, no correlation could be observed between carbon atoms and N resonating at -356 ppm, that could indicate either that these N atoms are involved in heterocyclic structures or that they are isolated within N-rich structures. Ammonium or hydrazinium compensat-

ing negatively charged polynitrogen moieties might be good candidates. The free rotation of the NH_4^+ group results in a poor efficiency of the ^1H – ^{15}N magnetisation transfer. It should also be noted that nitriles are not clearly visible in these 2D spectra because their detection requires longer t_{CP1} (≥ 10 ms) than those used in the 2D experiments.

3.4. Discussion

This comprehensive NMR study has allowed the elucidation and confirmation of structural units and functional groups that have been suggested to be present within tholins from other techniques, especially the presence of nitriles. Characteristic nitrile ($\text{C}\equiv\text{N}$) stretching vibrations were observed by FTIR (Khare et al., 2002; McDonald et al., 1994; Sarker et al., 2003; Imanaka et al., 2004; Quirico et al., 2008) and Raman spectroscopy (Imanaka et al., 2004; Bernard et al., 2006; Szopa et al., 2006; Quirico et al., 2008). Various compounds and molecular fragments containing a nitrile group were released upon pyrolysis (Ehrenfreund et al., 1995; Coll et al., 1999; Hodyss, 2005; Szopa et al., 2006; McGuigan et al., 2006). Mass spectrometry results on the tholin soluble fraction report losses of HCN, indicative of the presence of nitrile functions (Sarker et al., 2003; Hodyss, 2005). Various oligomeric aminonitrile units ($\text{CN}-(\text{CH}_2)_x-\text{NH}_2$) were proposed to constitute structural units of tholins based on mass spectrometric studies (Hodyss, 2005; Pernot et al., 2010).

The contribution of aminonitriles implies the presence of amino groups that have also been detected by FTIR spectra (Khare et al., 2002; McDonald et al., 1994; Sarker et al., 2003; Imanaka et al., 2004; Quirico et al., 2008). However the precise nature (primary or secondary) of the species could not be specified. D–H exchange experiments in solution also support the presence of amino (or imino) functions (Somogyi et al., 2005). From the present study, several types of amino groups may contribute to the chemical structure of tholins. No direct evidence for amino groups linked to aliphatic carbons can be derived from the 2D NMR spectra; however, their occurrence is strongly suggested by the observations in the 1D double CP experiments. This might at first appear at variance with the discussion and conclusions of Quirico et al. (2008). However, the amino group in arylcyanoguanidines **VIII** has a chemical shift around -300 ppm and it is linked to an imino carbon which resonates at 160 ppm in ^{13}C NMR (Cunningham and Wan, 1996). Guanidine **IX** and biguanide **X** have been proposed as “chemical roots” for the methanol soluble fraction of tholin based on ESI analyses (Pernot et al., 2010). The present double CP experiments suggest the coupling of nitrogen resonating at -280 ppm with a cyano group. In addition, a correlation is observed between ^{15}N at -280 ppm and ^{13}C at 168 ppm. Based on their chemical shifts, these N and C species may belong to an imino group suggesting the occurrence of a $\text{C}=\text{N}-\text{C}\equiv\text{N}$ moiety as in **VIII**. The presence of imino groups has already been inferred from FTIR spectroscopy (McDonald et al., 1994; Sarker et al., 2003).

Another type of amino group that cannot be excluded is the case of amino groups attached to C atoms contained within heterocyclic structures. Their chemical shift values occur at around -300 ppm and they are linked to C atoms for which the shifts occur in the 160 – 170 ppm range. The adjacent N atoms show chemical shifts at around -180 ppm due to amino substitution of the carbon atoms. Our double CP experiment clearly shows a correlation between ^{13}C at 168 ppm and ^{15}N at -280 and -174 ppm, in agreement with such a sub-structure. The presence of heterocycles in tholins was suggested by pyrolysis studies as well as by UV Raman spectroscopy and FTIR (Ehrenfreund et al.,

1995; Pietrogrande et al., 2001; Khare et al., 2002; Imanaka et al., 2004; Hodyss, 2005; McGuigan et al., 2006; Quirico et al., 2008). Interestingly, the $\text{C}=\text{N}-\text{C}\equiv\text{N}$ moiety can be related to such a heterocyclic structure, as dicyandiamine **XI** is known to be readily converted into melamine and melem by heating (Belsky et al., 1997).

As far as we know, ammonium and hydrazinium ions have not been considered so far in elucidating the chemical structure of tholins. However, the present NMR results suggest their existence close to a negatively charged nitrogen-rich moiety in the model tholin material studied here.

Aromatic hydrocarbon moieties were also proposed from pyrolysis studies to contribute to the chemical structure of tholins (Ehrenfreund et al., 1995; Pietrogrande et al., 2001; Coll et al., 1999; Szopa et al., 2006; McGuigan et al., 2006). The low intensity of the signal around 130 ppm in ^{13}C NMR and its behaviour in the variable contact time experiment points to a lack of protonated aromatic carbons in agreement with previous FTIR observations (Quirico et al., 2008).

Occurrence of isocyano groups in tholins was suggested from FTIR data (Imanaka et al., 2004; Quirico et al., 2008). However, the isocyano groups are characterized by resonances at 160 ppm for ^{13}C and -200 ppm for ^{15}N . Signals are observed in these regions in each CP/MAS spectrum but double CP experiments could not reveal any correlation between these two signals. The isocyano contribution must therefore be considered to be minor in the tholin.

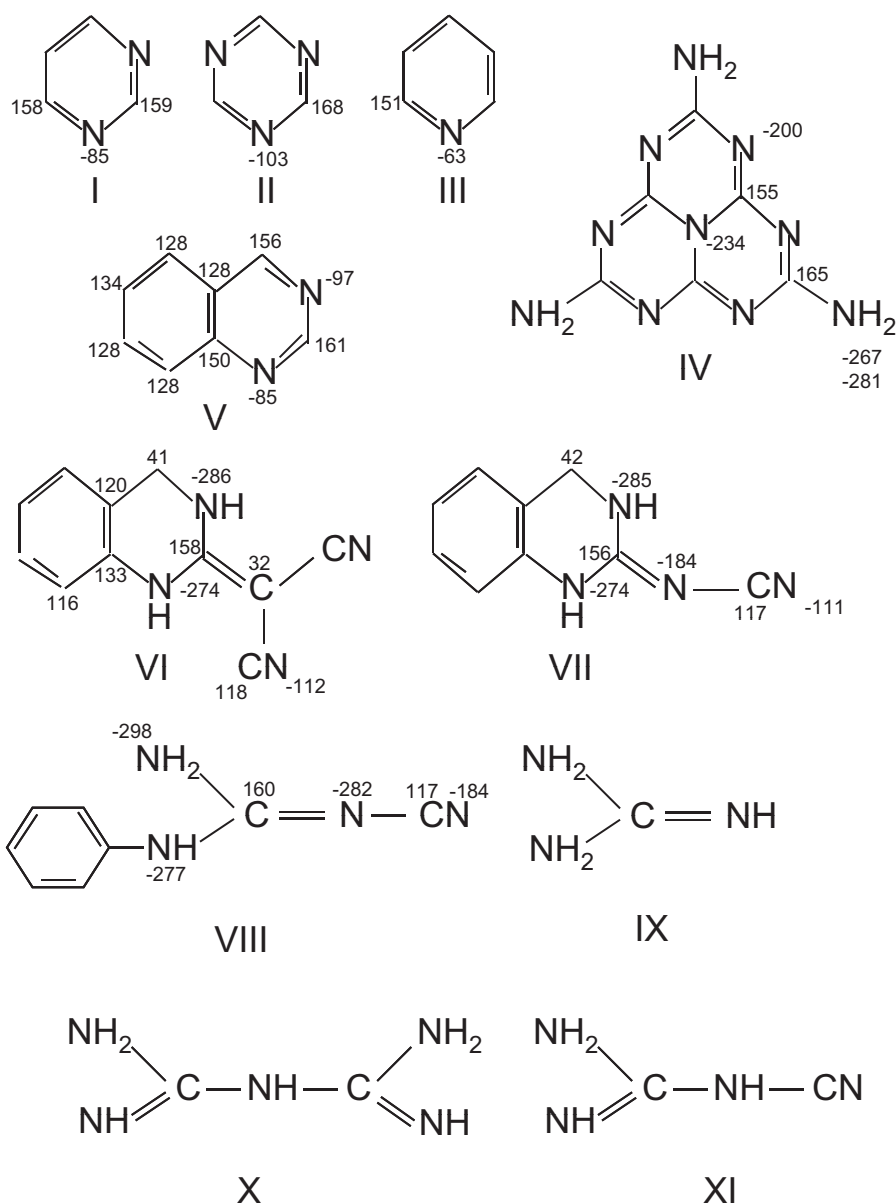
Several other species and structural groups have also been proposed to be present in tholins according to FTIR (Imanaka et al., 2004) but the present study has shown that if they are present, it can only be in minimal quantities. For example, carbodiimide moieties ($\text{N}=\text{C}=\text{N}$) could give rise to ^{15}N chemical shifts at around -280 ppm, but ^{13}C in these structures would resonate at 140 ppm, where no obvious NMR signal is observed. Hydrazines ($\text{R}_1\text{R}_2\text{N}-\text{NR}_3\text{R}_4$) are characterized by ^{15}N and ^{13}C chemical shifts at -275 to -330 ppm and 150 ppm respectively. The low abundance of the ^{13}C signal in this latter range rules out a major contribution from these species. Contribution of hydrazones ($\text{R}_1\text{R}_2\text{N}=\text{CR}_3\text{R}_4$) was previously excluded from the analysis of the FTIR spectrum (Quirico et al., 2008) and this is confirmed by the present NMR study because the chemical shift of the N atoms involved in the imino bond would occur at ca. -20 ppm. Similarly, diazo compounds ($\text{R}_1\text{R}_2\text{C}=\text{N}=\text{N}$) can be excluded because the terminal nitrogen is strongly deshielded (-5 to -65 ppm).

In conclusion, the present ^{13}C and ^{15}N NMR study combined with the first principles electronic structure calculation results indicate that the model tholin structure is mainly based on unsaturated C–N bonded units, contained within sp^2 bonded species such as imines or aromatic triazine or heptazine units, or nitrile ($-\text{C}\equiv\text{N}$) groups. Amino groups ($-\text{NH}_2$) are also present, most likely linked to sp^2 -bonded C as are some methyl ($-\text{CH}_3$) groups. Along with previous mass spectrometry and FTIR, UV–visible and FT-Raman investigations, this places additional and new constraints on the likely structures and compositions of the Titan's tholins.

Acknowledgments

The authors acknowledge the exobiology program of the French space agency (CNES) for financial support. The French Région Ile de France SESAME program is acknowledged for financial support (700 MHz spectrometer). P.F.M., F.C. and C.P. are supported by the UK EPSRC.

Appendix A



References

- Aliev, A.E. et al., 2011. High-resolution solid-state²H NMR spectroscopy of polymorphs of glycine. *J. Phys. Chem. A* 115, 12201–12211.
- Belsky, A.J., Li, T.-J., Brill, T.B., 1997. Reactions of cyanamide, dicyandiamide and related cyclic azines in high temperature water. *J. Supercrit. Fluids* 10, 201–208.
- Benassi, R. et al., 2000. Exocyclic push-pull conjugated compounds. Part 3. An experimental NMR and theoretical MO ab initio study of the structure, the electronic properties and barriers to rotation about the exocyclic partial double bond in 2-exo-methylene and 2-cyanoimino-quinazolines and -benzodiazepines. *J. Mol. Struct.* 520, 273–294.
- Bernard, J.M., Quirico, E., Brissaud, O., Montagnac, G., Reynard, B., McMillan, P., Coll, P., Nguyen, M.-J., Raulin, F., Schmitt, B., 2006. Reflectance spectra and chemical structure of Titan's tholins: Application to the analysis of Cassini-Huygens observations. *Icarus* 185, 301–307.
- Bojdys, M.J., Muller, J.-O., Antonietti, M., Thomas, A., 2008. Ionothermal synthesis of crystalline, condensed, graphitic carbon nitride. *Chem. Eur. J.* 14, 8177–8182.
- Cardamone, J.M., Nuñez, A., Ashby, R., Dudley, R., 2006. Activated peroxide for enzymatic control of wool shrinkage. Part I: Elucidation. *Textile Res. J.* 76, 99–108.
- Carrasco, N. et al., 2009. Chemical characterization of Titan's tholins: Solubility, morphology and molecular structure revisited. *J. Phys. Chem. A* 113, 11195–11203.
- Clark, S.J. et al., 2005. First principles methods using CASTEP. *Z. Kristallogr.* 220, 567–570.
- Coll, P., Guillemin, J.-C., Gazeau, M.-C., Raulin, F., 1999. Report and implications of the first observation of C₄N₂ in laboratory simulations of Titan's atmosphere. *Planet. Space Sci.* 47, 1433–1440.
- Cunningham, I.D., Wan, N.C., 1996. ¹³C and ¹⁵N NMR study of electron distribution in *N*-aryl-*N'*-cyanoguanidines. *Magn. Res. Chem.* 34, 221–226.
- Ehrenfreund, P., Boon, J.J., Commandeur, J., Sagan, C., Thompson, W.R., Khare, B., 1995. Analytical pyrolysis experiments of Titan aerosol analogues in preparation for the Cassini Huygens mission. *Adv. Space Res.* 15, 335–342.
- Frisch, M.J. et al., 2009. Gaussian 09. Revision A.02. Gaussian, Inc., Wallingford, CT.
- Fujiwara, T., Sugase, K., Kainosho, M., Ono, A., Ono, A., Akutsu, H., 1995. C-13–C-13 and C-13–N-15 dipolar correlation NMR of uniformly labeled organic-solids for the complete assignment of their C-13 and N-15 signals—An application to adenosine. *J. Am. Chem. Soc.* 117, 11351–11352.
- Ganesan, A.L., Brinckerhoff, W.B., Coll, P., Nguyen, M.-J., Cornish, T.J., Ecelberger, S.A., 2007. Analysis of Titan tholins by laser desorption mass spectrometry. *Lunar Planet. Sci.* XXXVIII (abstract).
- Hodyss, R., 2005. Methods for the Analysis of Organic Chemistry on Titan. Ph.D. California Institute of Technology, Pasadena, California.
- Imanaka, H., Smith, M.A., 2010. Formation of nitrogenated aerosols in the Titan upper atmosphere. *PNAS* 107, 12423–12428.

- Imanaka, H., Khare, B.N., Elsila, J.E., Bakes, E.L.O., McKay, C.P., Cruikshank, D.P., Sugita, S., Matsui, T., Zare, R.N., 2004. Laboratory experiments of Titan tholin formed in cold plasma at various pressures: Implications for nitrogen-containing polycyclic aromatic compounds in Titan haze. *Icarus* 168, 344–366.
- Jurgens, B., Irran, E., Senker, J., Kroll, P., Müller, H., Schnick, W., 2003. Melem (2,5,8-triamino-tri- s-triazine), an important intermediate during condensation of melamine rings to graphitic carbon nitride: Synthesis, structure determination by X-ray powder diffractometry, solid-state NMR, and theoretical studies. *J. Am. Chem. Soc.* 125, 10288–10300.
- Khare, B.N., Sagan, C., Arakawa, E.T., Suits, F., Callcott, T.A., Williams, M.W., 1984a. Optical constants of organic tholins produced in a simulated Titanian atmosphere: From soft X-ray to microwave frequencies. *Icarus* 60, 127–137.
- Khare, B.N. et al., 1984b. The organic aerosols of Titan. *Adv. Space Res.* 4, 59–68.
- Khare, B.N., Bakes, E.L.O., Imanaka, H., 2002. Analysis of the time-dependent chemical evolution of Titan Haze Tholin. *Icarus* 160, 172–182.
- Klapötke, T.M., Stierstorfer, J., 2009. The CN₇ anion. *J. Am. Chem. Soc.* 131, 1122–1134.
- Klapötke, T.M., Minar, N.K., Stierstorfer, J., 2009. Investigations of bis(methyltetrazolyl)triazenes as nitrogen-rich ingredients in solid rocket propellants – Synthesis, characterization and properties. *Polyhedron* 28, 13–26.
- Martin, G.J., Martin, M.L., Gouesnard, J.-P., 1981. ¹⁵N-NMR Spectroscopy. Springer-Verlag, Berlin, Heidelberg, Germany.
- Massiot, D. et al., 2002. Modelling one and two-dimensional solid-state NMR spectra. *Magn. Reson. Chem.* 40, 70–76.
- McDonald, G.D., Thompson, W.R., Heinrich, M., Khare, B.N., Sagan, C., 1994. Chemical investigation of Titan and Triton tholins. *Icarus* 108, 137–145.
- McGuigan, M., Waite, J.H., Imanaka, H., Sacks, R.D., 2006. Analysis of Titan tholin pyrolysis products by comprehensive two-dimensional gas chromatography-time-of-flight mass spectrometry. *J. Chromatogr. A* 1132, 280–288.
- McMillan, P.F. et al., 2009. Graphitic carbon nitride C₆N₉H₃HCl: Characterisation by UV and near-IR FT Raman spectroscopy. *J. Solid State Chem.* 182, 2670–2677.
- Neish, C.D., Somogyi, A., Lunine, J.I., Smith, M.A., 2009. Low temperature hydrolysis of laboratory tholins in ammonia–water solutions: Implications for prebiotic chemistry on Titan. *Icarus* 201, 412–421.
- Perdew, J.P., Burke, K., Ernzerhof, M., 1999. Generalized gradient approximation made simple. *Phys. Rev. Lett.* 77, 3865–3868.
- Pernot, P., Carrasco, N., Thissen, R., Schmitz-Afonso, I., 2010. Tholinomics—Chemical analysis of nitrogen-rich polymers. *Anal. Chem.* 82, 1371–1380.
- Pickard, C.J., Mauri, F., 2001. All-electron magnetic response with pseudopotentials: NMR chemical shifts. *Phys. Rev. B* 63, 245101–245113.
- Pietrogrande, M.C., Coll, P., Sternberg, R., Szopa, C., Navarro-Gonzalez, R., Vidal-Madjar, C., Dondi, F., 2001. Analysis of complex mixtures recovered from space missions. Statistical approach to the study of Titan atmosphere analogues (tholins). *J. Chrom. A* 939, 69–77.
- Pilling, S., Andrade, D.P.P., Neto, Á.C., Rittner, R., Naves de Brito, A., 2009. DNA nucleobase synthesis at Titan atmosphere analog by soft X-rays. *J. Phys. Chem. A* 113, 11161–11166.
- Quirico, E., Montagnac, G., Lees, V., McMillan, P., Szopa, C., Cernogora, G., Rouzaud, J.-N., Simon, P., Bernard, J.-M., Coll, P., Fray, N., Minard, R.D., Raulin, F., Reynard, B., Schmitt, B., 2008. New experimental constraints on the composition and structure of tholins. *Icarus* 198, 218–231.
- Ruiz-Bermejo, M., Menor-Salván, C., Mateo-Martí, E., Osuna-Esteban, S., Martín-Gago, J.Á., Veintemillas-Verdaguer, S., 2008. CH₄/N₂/H₂-spark hydrophobic tholins: A systematic approach to the characterisation of tholins. *Icarus* 198, 232–241.
- Ruiz-Bermejo, M., Menor-Salván, C., de la Fuente, J.L., Mateo-Martí, E., Osuna-Esteban, S., Martín-Gago, J.Á., Veintemillas-Verdaguer, S., 2009. CH₄/N₂/H₂-spark hydrophobic tholins: A systematic approach to the characterisation of tholins. Part II. *Icarus* 204, 672–680.
- Sagan, C., Khare, B.N., 1979. Tholins: Organic chemistry of interstellar grains and gas. *Nature* 277, 102–107.
- Sagan, C., Khare, B.N., Thompson, W.R., McDonald, G.D., Wing, M.R., Bada, J.L., Vo-Dinh, T., Arakawa, E.T., 1993. Polycyclic aromatic hydrocarbons in the atmospheres of Titan and Jupiter. *Astrophys. J.* 414, 399–405.
- Sarker, N., Somogyi, A., Lunine, J.I., Smith, M., 2003. Titan aerosol analogues: Analysis of the non volatile tholins. *Astrobiology* 3, 719–726.
- Schaefer, J., Stejskal, E.O., 1976. Carbon-13 nuclear magnetic resonance of polymers spinning at magic angle. *J. Am. Chem. Soc.* 98, 1031–1032.
- Schaefer, J., McKay, R.A., Stejskal, E.O., 1979. Double-cross-polarization NMR of solids. *J. Magn. Reson.* 34, 443–447.
- Somogyi, A., Oh, C.-H., Smith, M.A., Lunine, J.I., 2005. Organic environments on Saturn's moon, Titan: Simulating chemical reactions and analyzing products by FT-ICR and ion-trap mass spectrometry. *J. Am. Soc. Mass Spectrom.* 16, 850–859.
- Stothers, J.B., 1972. Carbon-13 NMR Spectroscopy. Academic Press, New York, USA.
- Szopa, C., Cernogora, G., Boufendi, L., Correia, J.J., Coll, P., 2006. PAMPRE: A dusty plasma experiment for Titan's tholins production and study. *Planet. Space Sci.* 54, 394–404.
- Thompson, W.R., Sagan, C., 1989. Atmospheric formation of organic heteropolymers from N₂ + CH₄: Structural suggestions for amino acid and oligomer precursors. *Origins Life* 19, 503–504.
- Vanderbilt, D., 1990. Soft self consistent pseudopotentials in a generalised eigenvalue formalism. *Phys. Rev. B* 41, 7892–7895.
- Waite, J.H., Young, D.T., Cravens, T.E., Coates, A.J., Crary, F.J., Magee, B., Westlake, J., 2007. The process of tholin formation in Titan's upper atmosphere. *Science* 316, 870–875.
- Wang, X., Maeda, K., Thomas, A., Takanahe, K., Xin, G., Carlsson, J.M., Domen, K., Antonietti, M., 2009. A metal-free polymeric photocatalyst for hydrogen production from water under visible light. *Nat. Mater.* 8, 76–80.
- Yates, J.R., Pickard, C.J., Mauri, F., 2007. Ultrasoft pseudopotentials. *Phys. Rev. B* 76, 24401–24411.
- Zhang, Z., Leinenweber, K., Bauer, M., Garvie, L.A.J., McMillan, P.F., Wolf, G.H., 2001. High-pressure bulk synthesis of crystalline C₆N₉H₃HCl: A novel C₃N₄ graphitic derivative. *J. Am. Chem. Soc.* 123, 7788–7796.